Synthesis and Characterization of CuO nanoparticles Using Morus, Citrus and Gossypium Plants Extract and Antibacterial Activities

Khairiah Qaid Al-Majdad*[1]*, Bakeel Ali Radman*[2]*, Sadiq Al- jabhah , Maha Al-Bahree , Elham Abu benah,and F. Yehya*[3]**

1 Department of Physics, Faculty of Science and Education, Albaydha university, Yemen.
2 Department of Biology, Faculty of Science and Education, Albaydha university, Yemen.
3 Department of Biology, Faculty of Science and Education, Albaydha university, Yemen.
**Corresponding Auther Email: Fahembajash@gmail.com*
DOI: https://doi.org/10.56807/buj.v4i2.309

Abstract

Copper oxide (CuO) nanoparticles (NPs) were synthesized biological methods using aqueous extract of leaves of Morus, Citrus, and Gossypium. Leaves as a reducing and capping agent. The advantages of this methods are simple operation, use of cheap, natural, nontoxic and benign precursors, absence of toxic reagents and mild and environmentally friendly conditions. The green synthesized CuO NPs was characterized by X-ray diffraction (XRD) analysis demonstrated that the CuO NPs were crystalline with a mono clinic structure. The formation of NPs is monitored by recording the UV –vis optical properties exhibits in UV - region and band gap energy (Eg) greater than 3 eV. Electrical conductivity increases when temperature increases during the synthesis. Antibacterial study of the CuNPs was established using both gram positive and gram negative pathogens.
Keywords :*Biological methods, CuO nanoparticles, Extract, Antibacterial.*

1. **Introduction**

Nanotechnology plays a very important role in modern research, it is the most capable technology that can be applied almost all fields such as pharmaceutical, electronics, health care, food and feed, biomedical science, drug and gene delivery, chemical industry, energy science, cosmetics, environmental health, mechanics and space industries. It has also been utilized for the treatments of infection, cancer, allergy, diabetes and inflammation (Alvarez *et al*.,2021; Saranyaadevi *et al*.,2014).

copper oxide nanoparticles (CuO NPs) is most widely used material in the world due to their electrical, optical, catalytic, mechanical and thermal, conduction properties, biomedical and antifungal/antibacterial. (Guin *et al*.,2015 ; Oruç and Altındal ,2017),

CuO NPs is one of the potential p-type semiconductors. The bandgap of CuO NPs from 1.2 (bulk) to > 2eV (Amer and Awwad ., 2021; Dahrul *et al*.,2016 ; Mari *et al*.,2020 ; Rao *et al*.,2009), due to the quantum confinement effect (Radhakrishnan and Beena,2014). CuO NPs is highly toxic to microorganism such as bacteria (*E-Coli*, *Staphylococcus Aureus*, *Pseudomonas aeruginosa*) and non-toxic to animal cells, due to these phenomena it is considered to be an effective bactericidal metal. Itis consider to bea safe for human beings such as food package and in water treatment. (Saranyaadevi *et al*.,2014) . Several methods are available for CuO NPs synthesize, namely, microwave irradiation, electrochemical (Borgohain *et al*.,2000), sol gel method (Dhaouadi *et al*.,2018), chemical reaction, solid state reaction (Vidyasagar *et al*.,2012) , and co-precipitation, However, chemical synthesis of CuO leads to the adsorption of toxic chemicals on its surface, which may have harmful effects when used in biomedical applications (Shi *et al*.,2017). green synthesis method is one of the best method for the production of nanoparticles in recent years. This green synthesis method has several advantages over other methods namely cost effectiveness, simplicity, use of less temperature, eco-friendly, the usage of less toxic materials, moreover it is compatible for medical and food applications (Shah *et al*.,2015). CuO NPs have been synthesized by using Various plants extract from Various parts such as leaves, fruits, skin of the fruits, roots, seeds, barks, stem, peels and flowers (Amer and Awwad., 2021; Mari *et al*.,2020). synthesized CuO NPs using *Desmodium gangeticum* root extracts and explored its biological activity (Guin *et al*.,2015), Bougainvillea flowers (Shammout and Awwad.,2021), *Phoenix dactyliferous L* leaves (Berra *et al*.,2018), tea leaf and coffee powder extracts (Sutradhar *et al*., 2014). Leaves of *Azadirachta indica*, *Pongamia pinnata*, *Lantana camara* and orange peel *(Citrus reticulata)* (Shiny *et al*.,2019), *Adiantum lunulatum* whole plant extract (Sarkar *et al*.,2020), *Thymus vulgaris* L. leaves (Nasrollahzadeh *et al*.,2015),

The aim of the present study is to synthesize and characterize CuO nanoparticles by using Morus, Citrus, and Gossypium leaves extracts, followed by analysis structures, optical and electrical. Properties and antibacterial activities.

2. Material and Methods

2.1 Materials Chemical

All chemicals were analytical grade and were used without further purification. Copper(II) sulphate pentahydrate ($CuSO_4{\cdot}5H_2O$, 98.5%), sodium hydroxide (95%), ethanol (C_2H_5OH, 99.5%), and distilled water

2.2 Preparation of leaf extract

The leaves were thoroughly washed and rinsed with distilled water, and then finely cut. The leaves were then homogenized using mortar and pestle. The extraction was carried out by mixing 10 g of the grinded leaves with 100 ml of de-ionized water and was immediately stirred using magnetic stirrer and heated for about 10 minutes at a temperature of 70-80 °C. After wards, it was allowed to cool down to room temperature. The mixture was, firstly, filtered using Abron Qualitative filter paper and then using Quantitative filter paper, after which the collected filtrate was kept at 4 °C for further synthesis of CuO NPs (Gebremedhn *et al*.,2019).

2.3 Green synthesis of (CuO NPs)

CuO NPs were synthesized through a reduction of copper sulfate by the phenolic compounds of leaf extract. The reaction mixture was prepared by adding 10 ml of the plant extract to 100 ml of 0.02 M $CuSO_4.5H_2O$ solution in a 250 ml flask. The reaction was carried out using reflux mounting under continuous stirring at 60°C for 15 min, in this method simple involving the combination reaction between Copper sulfate pentahyate and leaves extract. Following, it was allowed to cool down. Afterwards, the mixture was treated with 1 M NaOH solution drop by drop for a specific pH = 10. The formation of CuO was confirmed by a color change from blue to dark green. To obtain the precipitate which was centrifuged at 4000 rpm for 15 min and then at room temperature and washed several times with absolute ethanol and distilled water. The collected precipitate was dried at 80 ℃ for 2 h, then it was grind using mortar and pestle to get a fine powder. Finally, the powder was annealed at 400 ℃ for 2 h to obtain pure CuO nanoparticles (Begum *et al*.,2019).

2.4 Characterization of (CuO NPs)

The structural properties of prepared samples have investigated using the X-ray diffraction (XRD) technique (XD-2 X-ray diffractometer using CuKα (λ = 1.54 Å) at 36 kV and 20 mA, China) in Yemeni Geological Survey and Minerals Resources Board (YGSMRB). The absorbance and transmittance spectra of samples were measured using a UV–VISIBLE spectrophotometer (SPECORD 200) at room temperature in the wavelength range of (190–1100 nm).

The electrical conductivity of Nano fluids was measured by digital mustimeter Pocket -size meter (Model: EC59). The temperature of the system was measured by digital mustimeter (Model: DM-97). The manually made entire electrical conductivity experimental setup image was shown in Fig 1. Primarily, the instrument was calibrated using base solvent (deionized water) repeating up to find the value of agreement with the standard value. The electrical conductivity studies of Nano fluids (CuO) were execution with respect to temperature (Ramalingam *et al*.,2020).

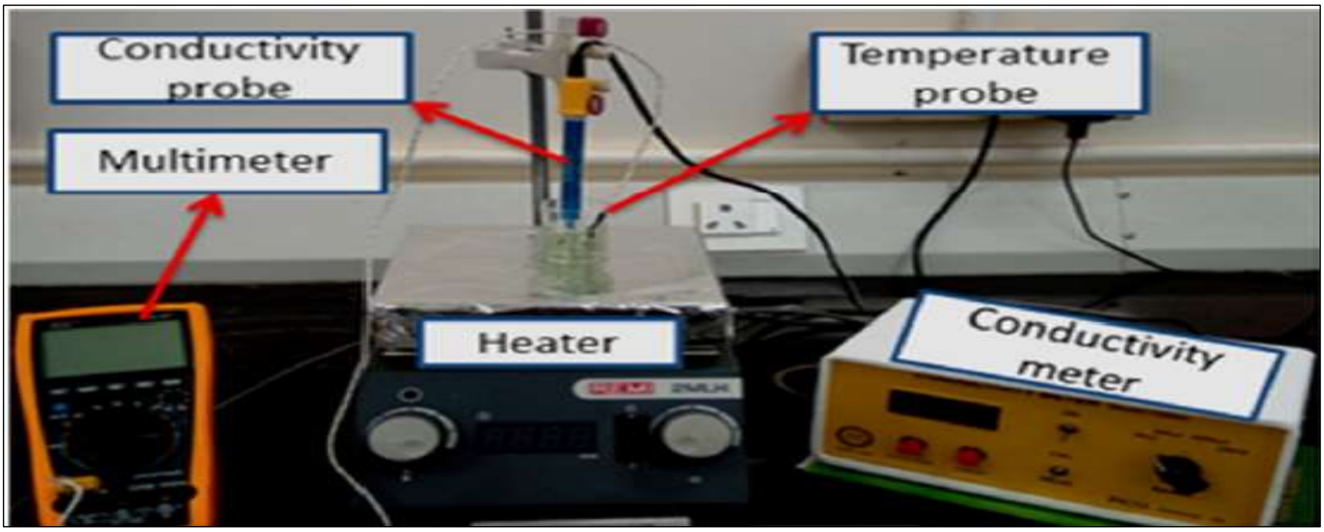

Fig. 1. Schematic images of electrical conductivity experimental (Ramalingam *et al.*,2020)

2.5. Antimicrobial Preparation

In first step, *Escherichia coli*, *Staphylococcus aureus* and *Klebsiella pneumoniae* have isolated and identified by Labinan Hospital Labs, Dhamar city. Then, we used o, b and c watery extract and o, b and c nanoparticle extracte concentrations 100% and 50 % which were put in media induced holes. After that, antibiotic (Tetracyclin, Vancomycin, Amikacin, Ceftriaxone and Azithromycine) were used. Inhibition zone siz were measure resistance (R) when no effect, moderate (M) which ranged between 1-3 mm and sensitive (S) which ranged between 4-7 and more when there is effect of bacterial growth.

2.6. Culture media and Antimicrobial assay

Mueller-Hinton agar (MH) (Hi-Media, Bombay, India) was respectively used for bacteria growth. Microbial cultures, freshly grown at 37°C the organisms were spread on MH agar plates by cotton swab. Antimicrobial activity was evaluated by measuring the inhibition zone size against the test organism (Kali *et al*., 2016).

3. Results and Discussion

3.1. structures properties

XRD patterns exhibited for CuO (M), CuO (C) and CuO (G). nanostructures as shown in Fig. 2. All presented samples showed three characteristic crystallographic. The configured diffraction peaks can be indexed to pure monoclinic structure crystalline phase, which are close enough to the standard values (JCPDS No: 48 -1548). The prominent diffraction peak values at 2θ = 32.51°, 35.42°, 38.91°, 48.71°, 56.81°, 61.52°, and 66.44° corresponding to $(\bar{1}10)$, $[\bar{1}11]$, (111), $[\bar{2}02]$, (020), (202) and $(\bar{1}13)$ planes respectively. These results from Eq. (1) for monoclinic structures by first calculating the lattices constant for more detail, see our previous published and the distance between the atoms in 2 dimensional (d) based on the Bragg equation. Crystallite size obtained using the Scherrer equation in Eq. (1), (Santhosh Kumar *et al*.,2020; Pavithran *et al*.,2020)

$$D = \frac{K\lambda}{\beta\cos(\theta)} \qquad (1)$$

$$\frac{1}{d^2} = \frac{1}{\sin^2\beta}\left[\left(\frac{h^2}{a^2} + \frac{k^2\sin^2\beta}{b^2} + \frac{D^2}{c^2} - \frac{2hl\cos\beta}{ac}\right)\right] \qquad (2)$$

$$\varepsilon = \left(\frac{1}{\sin\theta}\right)\left[\left(\frac{\lambda}{D}\right) - (\beta\cos\theta)\right] \qquad (3)$$

Where D is the average crystallite size (nm), K is the grain shape factor (0.9), λ is the X-ray wavelength (nm), β is the line broadening at half the maximum (FWHM) intensity in radians, and Θ is the Bragg diffraction angle of the 2Θ peak. The lattice parameters (a, b, c), and the strain (ε) of the obtained samples were estimated through the Eqs (2) and (3) (Raba-Pa´ez *et al*.,2020) and the results are presented in Table 1. (d) corresponds to the distance between the crystallography planes and h, k, l are the miller indices.

The dislocation density S listed therein was calculated using Eq. (4) and gives the measure of defects in crystalline structures (Chauhan *et al*.,2021)

$$S = \frac{1}{D^2} \qquad (4)$$

where D is the average crystallite size were

As shown in Table (1). The average crystallite size of CuO (M), CuO (C) and CuO (G) nanoparticles was found to be 38.51 ,30.32 and 42.79 nm respectively.

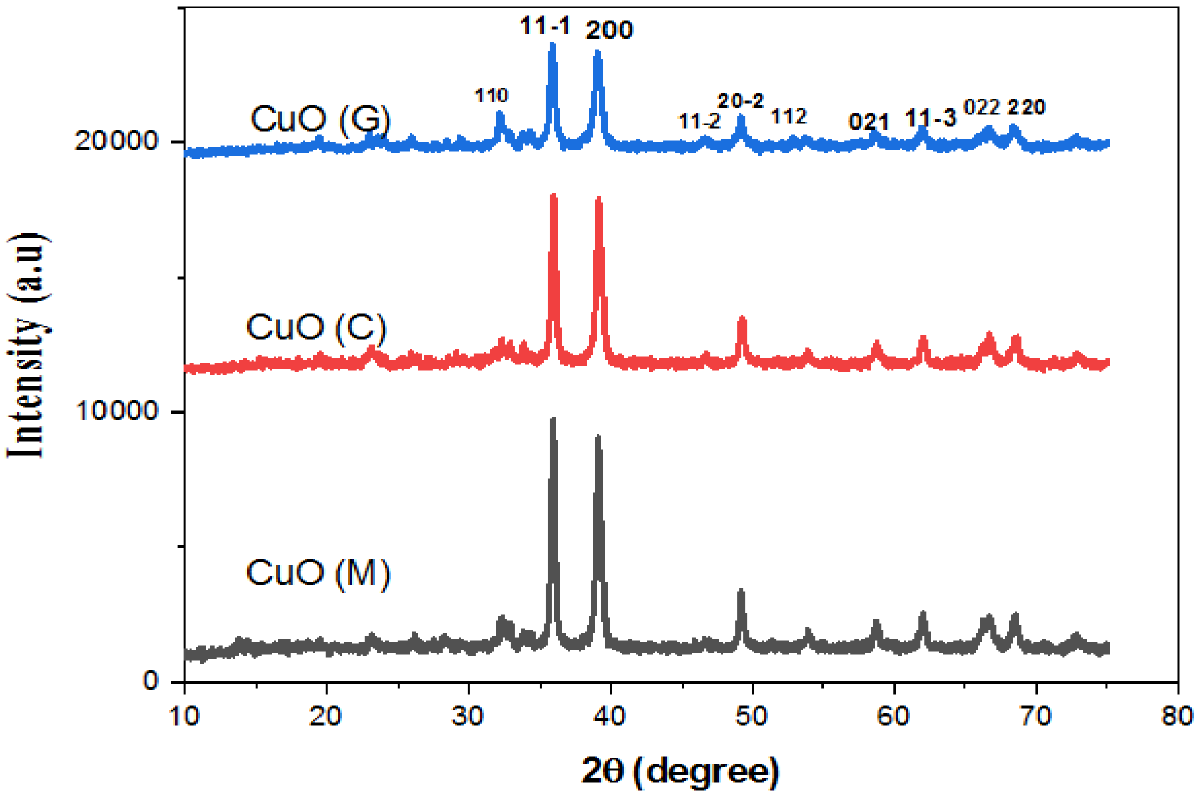

Fig. 2: X-ray diffraction (XRD) of green synthesized CuO nanoparticles (CuNPs).

Table (1) : Lattice Parameters , Average crystallite size, dislocation density, and macrostrain of CuO nanoparticles .

Samples	**Lattice Parameters (A°)**			**d(A°)**	**Average crystallites' size, D (nm)**	**Dislocation density, S × 10^{14} (line/m^2)**	**Macrostrain, ε × 10^{-3}**
	a	b	c				
CuO(G)	4.686	3.437	5.136	2.357	42.79	5.461	**1.073**
CuO(M)	4.695	3.428	5.141	2.302	38.51	4.144	**1.253**
CuO (C)	4.672	3.428	5.153	2.305	30.32	10.88	**0.689**

Dislocation density (S) is importance in the mechanical and structural properties of materials. The increase in the crystallite sizes is attributed to the small dislocation density value as in CuO (G) , because of the inverse relation between dislocation density parameters and crystallite size (Ahmed *et al.*,2021) .

3.2 Optical properties

3.2.1. Optical absorption study

The optical measurements are productive tools for understanding the band structure and evaluating the band gap width and optical parameters of both ordered and disordered materials (Elbashar *et al*.,2010). Fig 3a. demonstrates the absorption spectra CuO NPs a broad absorption band was observed at 263, 266 and 267 nm for CuO (M), CuO (C) and CuO (G) respectively.

The transmission spectra of all samples (Fig. 3(b)) has displayed almost an opposite behavior to that of absorption spectra. It was also observed that optical transmission increased in the Uv-region for three samples and has maximum value for CuO NPs. The increased in transmittance in Uv-region range is associated with the variation in crystallite size (size effect) and crystal defects.

explored a comparable transparency, absorbance for CuO which agreement range

with in published studies (Berra *et al.*,2018; Santhosh Kumar and VenkatKumar,2020; Shi *et al.*,2017). Our results are consistent

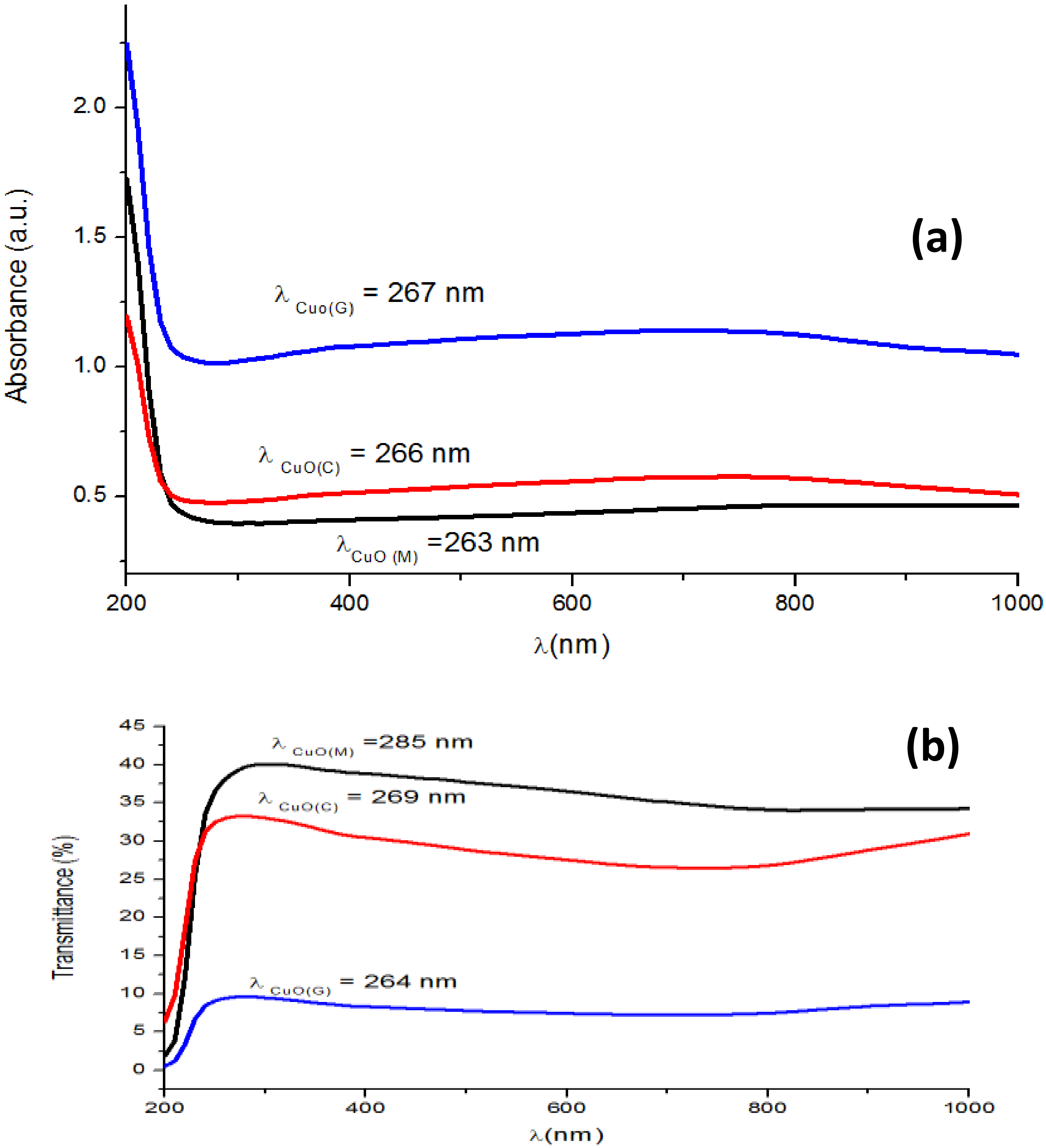

Fig. 3. (a) Absorbance and (b) Transmittance spectra of the prepared CuO nanostructures**.**

3.2.2. Bandgap determination

The fundamental absorption can be used for the estimation of optical bandgap (Eg) by using the relation between absorption coefficient(α) and incident photon energy (hυ) given by(Shariffudin *et al*.,2015):

$$(\alpha h\nu)^n = A(h\nu - E_g) \quad (6)$$

where, A is the characteristic parameter, υ is incident light frequency, h is Planck's constant and n is a power factor with value ½ for indirect and 2 for direct transition, and Eg is the optical band gap. extrapolation of the linear region of a plot of the graph of $(\alpha h\nu)^n$ on the y- axis versus photon energy (h υ) on the x – axis, gives the value of the optical band gap, Eg . (Abaker *et al* .,2011).

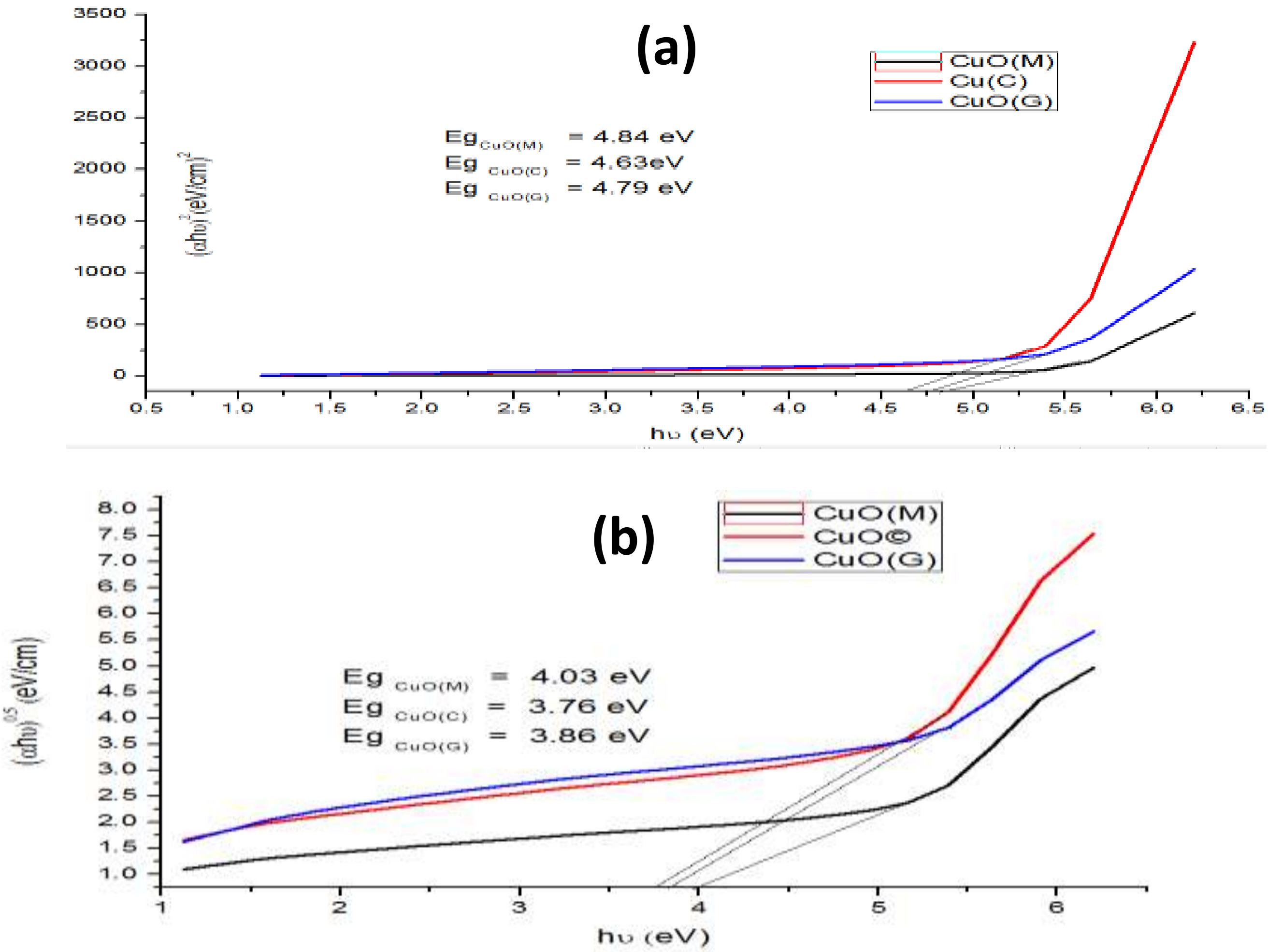

Fig. 4. Optical band gap energy (***Eg***) (a) direct transition semiconductor and (b) for indirect transition semiconductor.

Fig 4a shown the direct band gap (4.84,4.63 and 4.79) ev for CuO(M) ,CuO(C) and CuO(G) , and Fig 4b shown the indirect band gap (4.03,3.76 and 3.86) ev for CuO(M) ,CuO(C) and CuO(G) which direct and indirect are higher as compared to bulk values, this bule shift in direct and indirect band gab due to the quantum confinement effect (Radhakrishnan and beena,2014) . Value of band gap was in good agreement value with results published by (Elbashar *et al*.,2016 , Zayyoun *et al*.,2016).

3.4 Absorption coefficient

Absorption coefficient (α) is calculated using Beer-Lambert relation (Dahrul *et al*.,2016; Zayyoun *et al*.,2016)

$$\alpha = \frac{2.303A}{d} \quad or \quad \frac{1}{d} ln\left(\frac{1}{T}\right) \qquad (5)$$

Where α is the absorption coefficient in cm^{-1} , (d) is the thickness of the sample cell in centimeter (1cm). Fig.5 shows exponential decay of absorption coefficient with increasing wavelengths. Higher values of $\alpha > 1$ and 2.5 cm^{-1} correspond to a transition occurring between extended states in both conduction and valance bands, while region with lower values of $\alpha < 1$ and 2.5 cm^{-1} exhibits rough exponential behavior for CuO(M) ,CuO(C) and CuO(G)

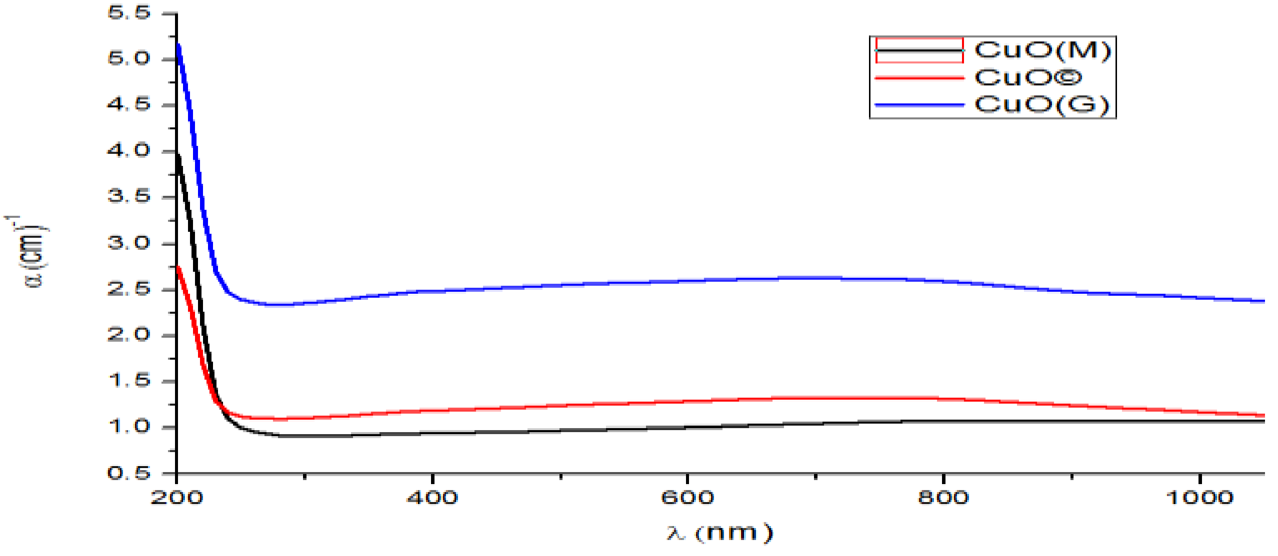

Fig. 5. Plot of absorption coefficient (α) as a function of wavelength of CuO

Refractive index (n) is an important parameter of optical materials, tells about the local fields, phase velocity of light and electronics polarization within the material. Refractive index (n) can be given by the (Kadham *et al.*,2017) :

$$n = \frac{1+\sqrt{R}}{1-\sqrt{R}} \qquad (7)$$

Extinction coefficient (k) or sometimes called absorption index is the amount of light lost due to absorption and scattering per unit distance in a testing material. The optical absorption coefficient (α) and incident photon wavelength (λ) can be used to calculate k given as

$$k = \frac{\alpha\lambda}{4\pi} \qquad (8)$$

The ***n*** and ***k*** as functions of wavelength (λ) provide an examination of the local field and ions electronic polarizability as shown in Fig. 6a and 6b, behavior of (k) and (n) with the incident photon wavelength for CuO sample of CuO (M) and CuO (C) the CuO(G) due to higher polarization of both Cu and O atoms in the CuO lattice matrix. Fig. 6b showed that the k value of CuO samples was the low indicated that CuO host lattice doesn't contain major defects. It is clearly seen that with the increased in the wavelength(λ), At the lower wavelength (maximum absorption region 200–300 nm equivalent to band edge) n and k have their maximum values referred to as anomalous dispersion.

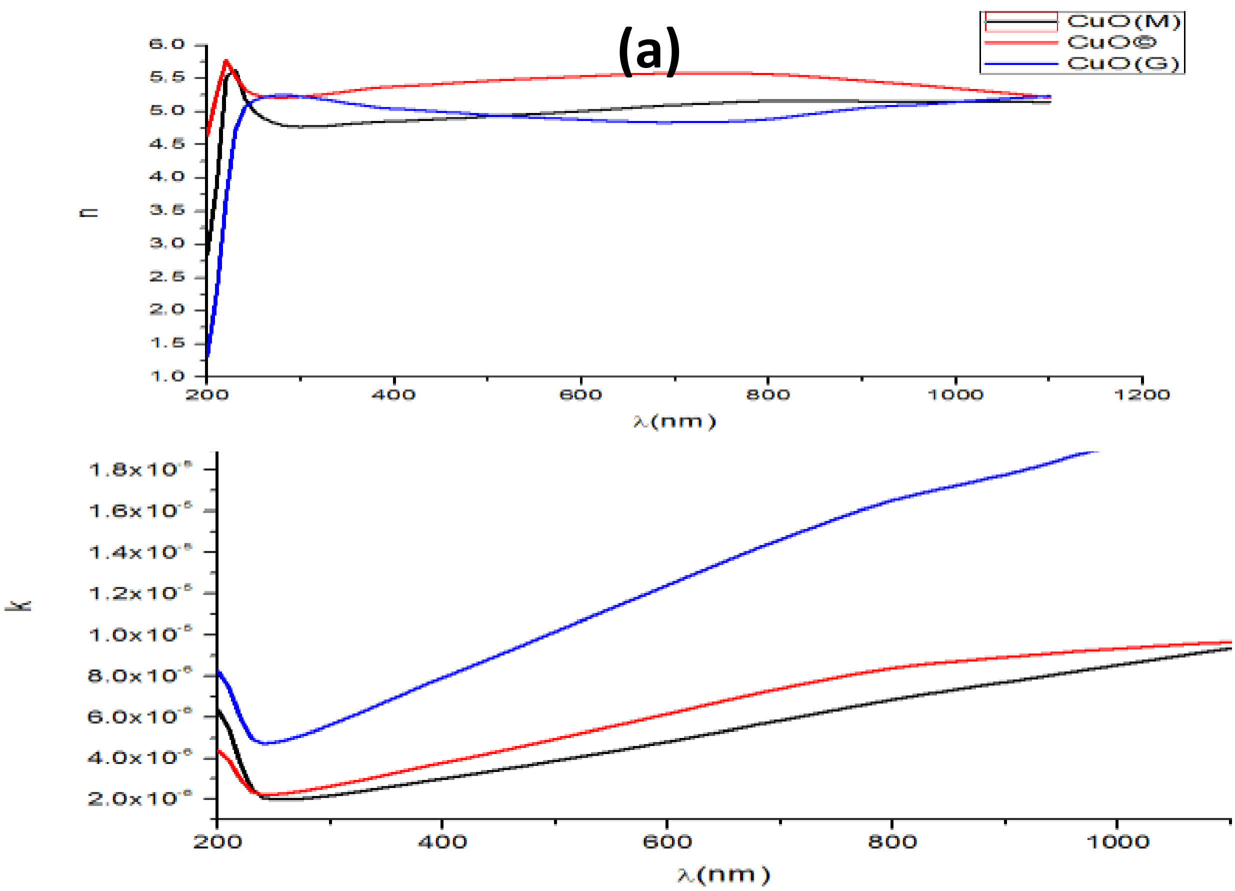

Fig. 6. (a) Refractive index (n), and (b) Absorption index (k) as a function of wavelength.

Fig6 (a and b) is also revealed that for nanoparticles there was no absorption in the long wavelength region (300–700 nm) suggested its normal dispersion behavior. Moreover, three peaks in k for nanoparticles was due to maximum absorption or fraction of light lost occurred at these points, also confirming three cupper oxides co-exist in a single phase.

3.2.4. Dielectric constant

Dielectric constant is a fundamental property of any oxides and it give information about polarizability and permittivity of a material associated with the density of states inside the forbidden gap. The real part (ε_1) of the dielectric constant shows the ability of material to slow down the speed of light and can be determined by using relation (Ahmed *et al*.,2021):

$$\varepsilon_1 = n^2 - k^2 \quad , \quad \varepsilon_2 = 2nk \qquad (9)$$

The imaginary part (ε_2) of the dielectric constant shows the absorption of energy (due to dipole motion) from an electric field and can be determined by using relation (9). Fig 7 (a-b) shows the change in real and imaginary parts of dielectric constant. It was found that real part of the dielectric constant for CuO NPs was change with photon energy and has a deep curve at 5.7 eV than sharply decreased in the high energy region. The imaginary part of the dielectric constant for CuO NPs was exponentially decreased in the high energy region with the highest, confirming the free carrier's contribution to the absorption.

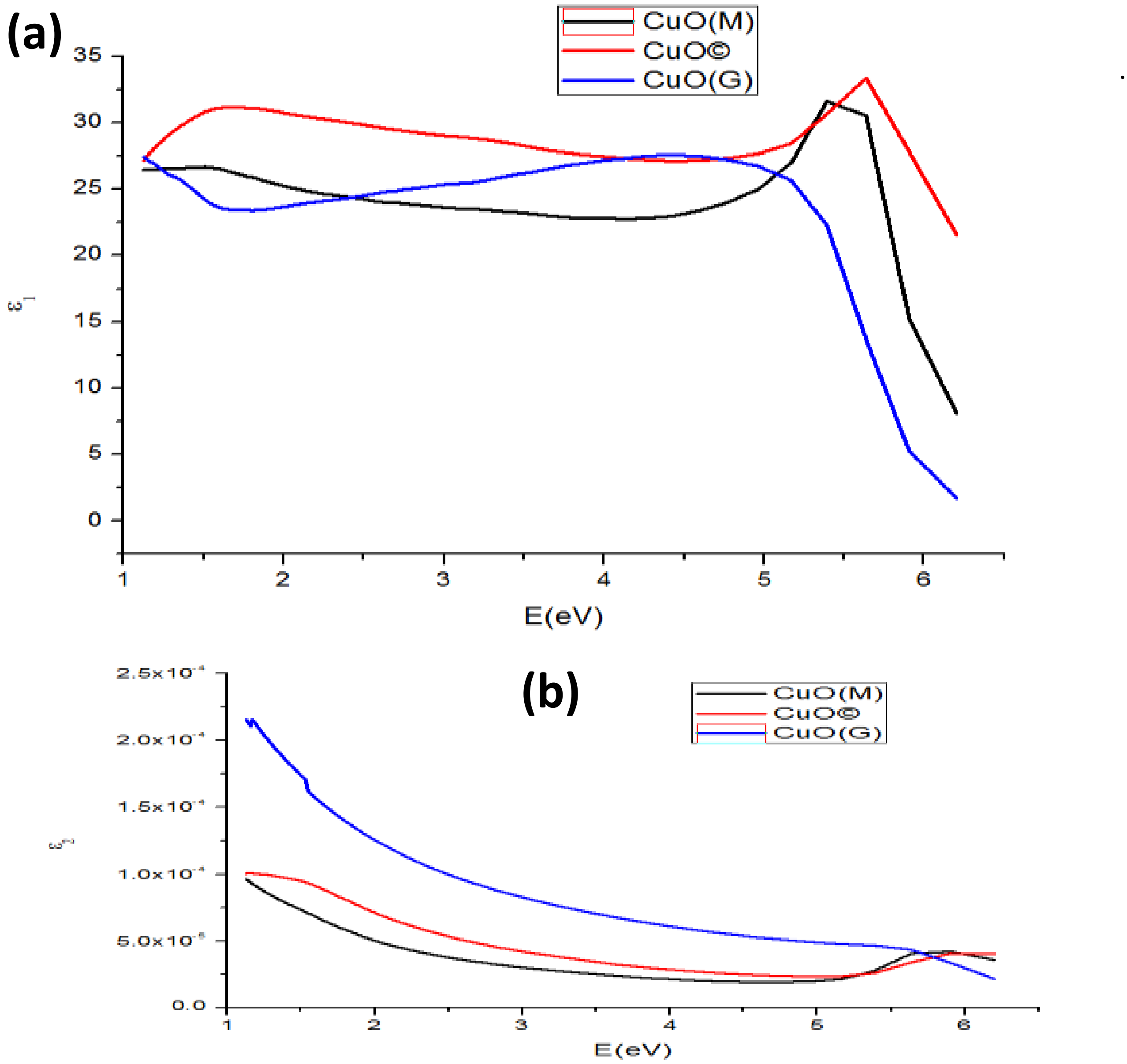

Fig. 7. The real (ε_1) (a) and imaginary (ε_2) (b) parts of the dielectric constant on the photon energy for CuO NPs .

3.2.5. Optical conductivity

The optical conductivity (σ_{opt}) is a vital parameter to study the optical behavior of material. The optical conductivity (σ_{opt}) of any material depends strongly on optical bandgap, absorption coefficient, extinction coefficient, incident photons frequency and the refractive index. Optical conductivity can be given as (Ahmed *et al.*,2021) :

$$\sigma_{opt} = \frac{\alpha n c}{4\pi} \qquad (10)$$

where c is the light velocity. Optical conductivity for CuO NPs are shown in Fig. 8 at high photon energy σ_{opt} was increased for CuO (M) and CuO (C) while σ_{opt} was decreased for CuO(G). The cause of this higher value of σ_{opt}, is the excitation of carriers from the valence band to the conduction band because of the greater nature of nanoparticles in this region. The higher value of σ_{opt} in Uv - region and absorbent has tremendous potential to be used as optical conducting material.

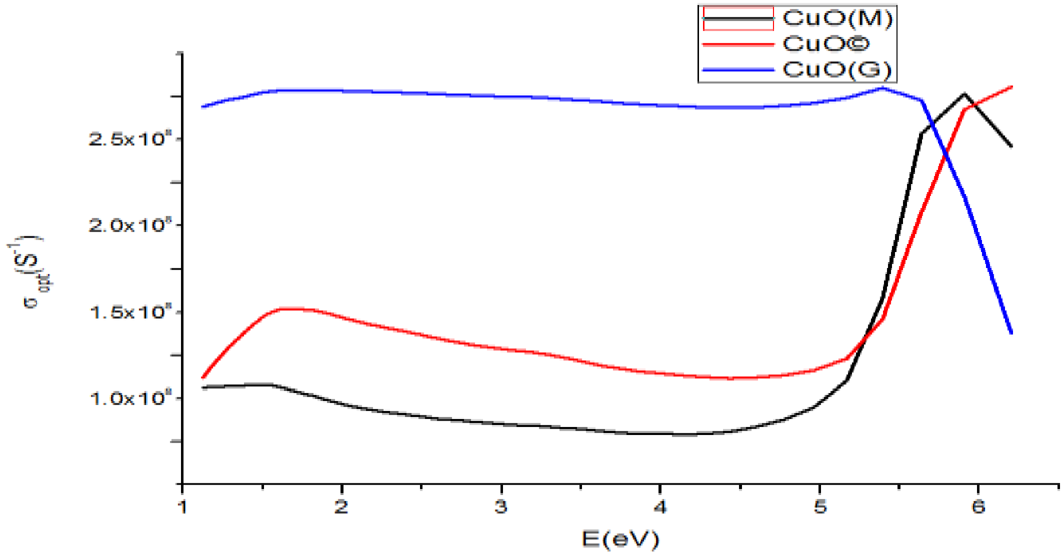

Fig. 8. Optical conductivity on the photon energy for the 3 prepared CuO PNs.

3. 3. Electrical Properties

Electrical conductivity (EC) assessment of Nano fluids comprising CuO nanoparticles water-based in (0.150g/l) concentrations, and various temperatures. Water as the base for Nano fluids preparation received increased attention from different research groups, mainly because of its large areas of applications. Furthermore, several outcomes on electrical conductivity of water-based Nano fluids (Minea,2019) The suspension with concentration of 0.150 g/l has been test for investigation of change temperature effects on electrical conductivity of CuO Nano fluids. Results are given in Table 2.

The authors revealed that electrical conductivity increase with the increase of temperatures such as EC for CuO(M) ≅ 1 .5 x10 $^{-3}$ to1 .6 x10 $^{-3}$ (S/cm) EC for CuO(C) ≅ 1 x10 $^{-3}$ (S/cm) and EC for CuO(G) ≅ 1 .1 x10 $^{-3}$ to1 .2 x10 $^{-3}$ (S/cm). Increase in temperature cause electrons that exist in valence electrons going to conductivity layer and participate in conductance or conductivity. (Azimi and Taheri,2015) . The increase of the EC with the increase of crystallite size indicates that the conduction mechanism is driven by grain boundary scattering. CuO were reported as p-type conductivity due to copper vacancies in the structure (Shariffudin *et al*.,2015). The presented results of the EC for the prepared samples are in good agreement with the literature (Grigore *et al*.,2016; Mohammed ,2014) and bigger then with the literature (Azimi and Taheri,2015).

3. 3. Antimicrobial

Culture assay of antibiotic sensitive test table 3 showed that, gram-positive bacteria (*Staphylococcus aureus*) is sensitive with Tetracycline and Amikacin, but resistance with Vancomycin, Ceftriaxone and Azithromycin. Gram-negative bacteria *Escherichia coli* showed sensitive with Amikacin, Ceftriaxone and Azithromycine. In addition, *Klebsiella pneumoniae* showed sensitive with Tetracyclin, Amikacin, Ceftriaxone and Azithromycine.

Table 3: Effect of antibiotic on bacteria growth

Gram stain	Positive	Negative	
Bacteria	*Staphylococcus aureus*	*Escherichia coli*	*Klebsiella pneumoniae*

Table 2: electrical conductivity of CuO NPs with temperature

Tetracyclin	S	R	S
Vancomycin	R	R	R
Amikacin	S	S	S
Ceftriaxone	R	S	S
Azithromycine	R	S	S

R=resistance when no effect. M= moderate ranged between 1-3 mm. S= sensitive which ranged between 4-7 and more

The watery extraction of Morus (M), Citrus © and Gossypium (G) do not effect on bacterial growth as shown in table 4

Table 4 : Effect of watery extraction of M., C .and G on bacteria growth

Gram stain	**Positive**	**Negative**	
Bacteria	*Staphylococcus aureus*	*Escherichia coli*	*Klebsiella pneumoniae*
M	R	R	R
C	R	R	R
G	R	R	R

R=resistance when no effect. M= moderate ranged between 1-3 mm. S= sensitive which ranged between 4-7 and more

The nanoparticle extraction of M, C and G table (5) showed that, CuO (M) 50 do not has effect on bacterial growth, but CuO (M) 100 has the same moderate effect on gram-positive and gram-negative. CuO (C) 100 has sensitive effect with gram-positive and gram-negative bacteria, but CuO (C) 50 has moderate effect on *Staphylococcus* aureus only. CuO (G) has no effect on *Staphylococcus aureus* growth, but has moderate effect on *Escherichia coli* and *Klebsiella pneumoniae*. CuO (G) 100 has sensitive effect on *Staphylococcus aureus*, *Escherichia coli* and *Klebsiella pneumoniae*.

Table 5: Effect of nanoparticles extraction of M, C.and G on bacteria growth

Gram stain	**Positive**	**Negative**	
Bacteria	*Staphylococcus aureus*	*Escherichia coli*	*Klebsiella pneumoniae*
CuO (M) 50	R	R	R
CuO (M) 100	M	M	M
CuO (C) 50	M	R	R
CuO (C) 100	S	S	S
CuO (G)50	R	M	M
CuO (G)100	S	S	S

R=resistance when no effect. M= moderate ranged between 1-3 mm. S= sensitive which ranged between 4-7 and more

4. Conclusions

The present study, reported a cost effective, eco-friendly and green approach method for synthesis of CuO NPs using aqueous extract of Morus, Citrus and Gossypiumleaves. XRD studies displayed that a synthesized nanoparticle exhibits a monoclinic crystalline structure having an average grain size of (42.79 ,38.51 and 30.32) nm for CuO (M), CuO (C) and CuO (G) respectively. The analytical tools like UV–

vis spectroscopy The results of the CuO NPs showed optical properties at UV – region and nanoparticles were effectively utilized for the antibacterial activity study.

Acknowledgements

The authors declare that they have no known competing financial interests or personal relationships that could have appeared to influence the work reported in this paper special Geniua University for sciences & Technoloogy.

References

A. Asha Radhakrishnan, B. Baskaran Been. (2014). Structural and Optical Absorption Analysis of CuO Nanoparticles. *Indian Journal of Advances in Chemical Science*, 2(2), 158-161.

Ankush Chauhan, Ritesh Verma, Khalid Mujasam Batoo , Swati Kumari, Rahul Kalia,, & Rajesh Kumar, Muhammad Hadi, Emad H. Raslan, Ahamad Imran. (2021). Structural and optical properties of copper oxide nanoparticles: A study of variation in structure and antibiotic activity. *Journal of Materials Research* 1-14.

Altındal, Çiğdem Oruç and Ahmet. (2017). Structural and dielectric properties of CuO nanoparticles. *Ceramics International*, 43(2017), 10708 - 10714.

A. Khawwam Mohammed. (2014). Studying the effect of Annealing on the Structural and Optical Properties of (Zn1-xFexO) Thin Films Prepared by Chemical Spray Pyrolysis Method, Thesis the Degree of M. Sc Diyala University, Iraq. ,

Anbuvannan Maria, Maria Vinosel Vincenta, Ramesh Mookkaiahb, Rajesh Subramanic, Kannadasan, & Nadesand. (2020). Catharanthus Roseus Leaf Extract Mediated Facile Green Synthesis of Copper Oxide Nanoparticles and Its Photocatalytic Activity. *Chemical Methodologies* ,4(2020), 424 - 436.

Awwad, Maisa'a W. Shammout and Akl M. (2021). A novel route for the synthesis of copper oxide nanoparticles using Bougainvillea plant flowers extract and antifungal activity evaluation. *Chemistry International, 7*(1), 71 -78.

Awwad, Mohammad W. Amer and Akl M. (2021). Green synthesis of copper nanoparticles by Citrus limon fruits extract, characterization and antibacterial activity. *Chemistry Interational, 7*(1), 1-8.

Alaa J. Kadham, Dalal Hassan, Najlaa Mohammad, Ahmed Hashim. (2018). Fabrication of (Polymer Blend-magnesium Oxide) Nanoparticle and Studying their Optical Properties for Optoelectronic Applications. *Bulletin of Electrical Engineering and Informatics, 7*(1), 28-34.

D. berra, S.E. Laouini, B. Benhaoua, M. R. Ouahrani,, & D. Berrani, A. Rahal. (2018). Green Synthesis of Copper Oxides Nanoparticles by Pheonix Dactylifera L Leaves Extract. *Digest Journal of Nanomaterials and Biostructures*, 13(4), 1231-1238.

C. C. Vidyasagar, Y. Arthoba Naik, T. G. Venkatesha, R. Viswanatha. (2012). Solid-State Synthesis and Effect of Temperature on Optical Properties of CuO Nanoparticles. *Nano-Micro Lett*, 4(2), 73 - 77.

G. Narsinga Rao, Y. D. Yao, and J. W. Chen. (2009). Evolution of size, morphology, and magnetic properties of CuO nanoparticles by thermal annealing. *J. Appl. Phys*, 105(093901).

G. Ramalingama, R. Vignesha, C. Ragupathib, C. Maria Magdalanec, K. Kaviyarasud,, & Kennedyd, J. (2020). Electrical and chemical stability of CuS nanofluids for conductivity of water soluble based nanocomposites. *Surfaces and Interfaces*, 19(2020), 1-7.

Hyo-Jeoung Lee, Jae Yong Song and Beom Soo Kim. (2013). Biological synthesis of copper nanoparticles using Magnolia kobus leaf extract and their antibacterial activity. *Research Article*, 1-7

Joy Sarkar , Nilanjan Chakraborty , Arindam Chatterjee , Avisek Bhattacharjee ,,, & Acharya, Disha Dasgupta and Krishnendu. (2020). Green Synthesized Copper Oxide Nanoparticles Ameliorate Defence and Antioxidant Enzymes in Lens culinaris. *Nanomaterials*, *10*(312), 1-27.

Kavita Borgohain , J. B. Singh, M. V. Rama Rao and T. Shripathi,Shailaja Mahamuni. (2000). Quantum size effects in CuO nanoparticles. *PHYSICAL REVIEW B*, 61(16), 11 093 - 011 096.

Kali, A., Devaraj B , P., Charles , M. & Seetha, K. S. (2016). Antibacterial synergy of curcumin with antibiotics against biofilm producing clinical bacterial isolates. Journal of basic and clinical pharmacy, 7, 93.

K. Saranyaadevi, V. Subha, R. S. Ernest Ravindran, S. Renganathan. (2014). Synthesis and Characterization of Copper Nanoparticle using Capparis Zeylanicaleaf Extract. *International Journal of ChemTech Research*, 6(10), 4533-4541.

K. S. Shiny, R. Sundararaj, N. Mamatha1, B. Lingappa. (2019). Anew approach to wood protection : prellminary study of biologically syntheized copper oxides nanoparticle formulation as an environmental friendy wood protectant against adecay fungi and termites. *Maderas. Ciencia y tecnología*, 21(3), 347 - 356.

Kiflom Gebremedhn, Mebrahtu Hagos Kahsay and Muluken Aklilu. (2019). Green Synthesis of CuO Nanoparticles Using Leaf Extract of Catha edulis and Its Antibacterial Activity. *Journal of Pharmacy and Pharmacology* ,7(2019), 327 -342.

Long-Bao Shi, Pei-Fu Tang, Wei Zhang, Yan-Peng Zhao, Li-Cheng Zhang and, & Zhang, Hao. (2017). Green synthesis of CuO nanoparticles using Cassia auriculata leaf extract and in vitro evaluation of them biocompatibility with rheumatoid arthritis macrophages (RAW 264.7). *Tropical Journal of Pharmaceutical Research January*, *16*(1), 185 -192.

Makeswari, S. Hemalatha and M. (2017). Green synthesis characterization and antibacterial studies of CuO nanoparticles from elchhornia crassipes. *R.I. Medical Journal*, *10*(8), 838 - 843.

Maiti, Prasanta Sutradhar • Mitali Saha • Debasish. (2014). Microwave synthesis of copper oxide nanoparticles using tea leaf and coffee powder extracts and its antibacterial activity. Nanostruct Chem, 4(86), 1-6.

Marissa Pérez-Alvarez , Gregorio Cadenas-Pliego , Odilia Pérez-Camacho ,, & Víctor E. Comparán-Padilla , Christian J. Cabello-Alvarado and Esmeralda Saucedo-Salazar. (2021). Green Synthesis of Copper Nanoparticles Using Cotton. *Polymers*, *13*(1906), 1-11.

Madalina Elena Grigore , Elena Ramona Biscu , Alina Maria Holban ,, & Monica Cartelle Gestal , and Alexandru Mihai Grumezescu. (2016). Methods of Synthesis, Properties and Biomedical Applications of CuO Nanoparticles. *Pharmaceuticals*, (Basel, Switzerland), 9(75), 2-14.

Mehdi Dhaouadi1, Mohamed Jlassi3, Imen Sta1, Islem Ben Miled, George Mousdis,, & Michael Kompitsas, Wissem Dimassi. (2018). Physical Properties of Copper Oxide Thin Films Prepared by Sol–Gel Spin–Coating Method. *American Journal of Physics and Applications*, 6(2), 43-50.

Mahmoud Nasrollahzadeh , S. Mohammad Sajadi , Akbar Rostami-Vartooni , Sarbast Mamand Hussin. (2016). Green synthesis of CuO nanoparticles using aqueous extract of Thymus vulgaris L. leaves and their catalytic performance for N-arylation of indoles and amines. *Journal of Colloid and Interface Science*, 466(2016), 113-119.

Minea, Alina Adriana. (2019). A Review on Electrical Conductivity of Nanoparticle-Enhanced Fluids. *Nanomaterials*, 9(1592), 1-22.

Monaliben Shah , Derek Fawcett , Shashi Sharma , Suraj Kumar Tripathy and, & Poinern, Gérrard Eddy Jai. (2015). Green Synthesis of Metallic Nanoparticles via Biological Entities. *Materials*, 8(2015), 7278–7308.

M Abaker, Ahmad Umar, S Baskoutas, S H Kim1 and S W Hwang. (2011). Structural and optical properties of CuO layered hexagonal discs synthesized by a low-temperature hydrothermal process. *Journal of physics D: Applied physics*, *44*(2011), 1-8.

M. Dahrula, Husin Alatasb, Irzaman. (2016). Preparation and optical properties study of CuO thin film as applied solar cell on LAPAN-IPB Satellite. *Procedia Environmental Sciences*, 33(2016), 661 – 667.

N. Zayyoun, B. Jaber, L. Laânab1, E. Ntsoenzok and R. Bekkari. (2016). Effect of solvent on the morphological and optical properties of CuO nanoparticles prepared by simple sol-gel process. *J. Mater. Environ*, 5(7), 1791-1797.

Rohit Guin, Shakila Banu A, Gino A Kurin. (2015). Synthesis of Copper Oxides Nanoparticles Using *Desmdium Gangeticum* Aqueous Root Extract. *International Journal of Pharmacy and Pharmaceutical Sciences*, 7(1), 1-6.

Raba-Pa´ezID, Angela Mercedes, 1, João Ota´vio D. Malafatti, Carlos Arturo Parra-, & Vargas, Elaine Cristina Paris, Miryam Rinco´ n-Joya. (2020). Effect of tungsten doping on the structural morphological and bactericidal properties of nanostructured CuO. PLOS ONE, 1-16

Santhoshkumar J, VenkatKumar Shanmugam. (2020). Green Synthesis of Copper Oxide Nanoparticles from Magnolia Champaca Floral Extract and its Antioxidant & Toxicity Assay using Danio Rerio. *International Journal of Recent Technology and Engineering (IJRTE)*, 8(5), 1-6.

Shakeel Ahmad Khan, Sammia Shahid, Muhammad Rizwan Sajid, Farah Noreen and Sadia Kanwal. (2017). Biogenic synthesis of CuO nanoparticles and their biomedical application: A current review. *Int. J. Adv. Res., 5*(6), 925-946.

Swathi Pavithran, Manikantan Pappuswamy, Yamuna Annadurai,, & Periyaswamy, Vijaya Anand Armugam and Thirunavukkarasu. (2020). Green Synthesis of Copper Nanoparticles, Characterization and Their Applications. *Journal of Applied Life Sciences International*, *23*(7), 10 -24.

S. Nazarath Begum, A. Esakkiraja, S. Mohamed Asan, M. Muthumari, G. Vembu Raj. (2019). Green Synthesis of Copper Oxide Nanoparticles Using Catharanthus Roseus Leaf Extract and Their Antibacterial Activity. *International Journal of Scientific Research*, 5(8), 21-27.

S.S. Shariffudin, S.S. Khalid, N.M. Sahat, M.S.P. Sarah, H. Hashim. (2015). Preparation and Characterization of Nanostructured CuO Thin Films using Sol-gel Dip Coating. *IOP Conf. Series: Materials Science and Engineering*, *99*(2015), 1-7.

Taheri, H. R. Azimi and R. (2015). Electrical conductivity of CuO nanofluids. *International Journal of Nano Dimension*, 6(1), 77 - 81.

Paul, Krishna Nama Manjunatha and Shashi. (2015). Investigation of Optical Properties of Nickel Oxide Thin Films Deposited on Different Substrates. *Accepted Manuscript*, 1 - 13

Yahia H. Elbashar, Ali M. Badr1, Haron A. Elshaikh1, Ahmed G. Mostafa, & Ibrahim, Ali M. (2016). Dielectric and optical properties of CuO containing sodium zinc phosphate glasses. *Processing and Application of Ceramics*, 10(4), 277–286.